Electronic structure of Si-skeleton materials

Kyozaburo Takeda and Kenji Shiraishi
Basic Research Laboratories, Nippon Telegraph and Telephone Corporation, 3-9-11 Midori-cho, Musashino-shi, Tokyo 180, Japan
(Received 9 January 1989)

The electronic structures of Si-skeleton chainlike [one-dimensional (1D)] and planar [two-dimensional (2D)] materials have been calculated by the first-principles local-density-functional method. 1D Si-skeleton material (chain polysilane) has a directly-allowed-type band structure with a band gap of about 4 eV. Interchain interaction disappears, independently of the chain configuration, if each chain is located over 8 Å from other chains. Therefore, the electronic structure of some polysilane-chain aggregations can be discussed in terms of the result for the corresponding isolated polysilane chain. 2D material (planar polysilane) has an indirect band gap of 2.48 eV as well as a direct band gap of 2.68 eV. This structure is an intermediary between direct (1D) and indirect (3D). A characteristic single, double, and treble degeneracy is found at the highest occupied valence-band state, depending on the structure dimension of 1D, 2D, or 3D Si skeleton, respectively.

I. INTRODUCTION

Si-skeleton materials have various characteristic structures; one-dimensional (1D) materials correspond to chainlike polysilanes, 2D materials are planar polysilane, and 3D materials are well-known crystalline Si and amorphous Si. Many 1D chainlike polysilanes have been synthesized. They are typical nonpolar high polymers, and have σ band-edge states. These states are formed of skeleton Si atomic orbitals (AO's) and are delocalized along the skeleton axis, similar to other nonpolar high polymers of normal alkanes. However, band gaps of polysilanes are half those of normal alkanes. Therefore, many experimental and theoretical studies[1,2] have been made for scientific interests and also technological applications such as photoresists in photolithography and photoconductors in photocopying processes. Conversely, 2D planar polysilane is still a hypothetical polymer. Only a prototype analogue has been recently reported.[3,4] However, this material is an important intermediary between 1D polysilane chains and 3D silicon materials.

We have theoretically calculated electronic structures of Si skeleton chainlike and planar high polymers, based on the first-principles local-density-functional (LDF) method. This paper compares the calculated electronic structure for an isolated chain with previous results.[5-10] Next, it theoretically discusses the influence on the electronic structure of interchain interaction in order to investigate how crystallization of polysilane chains influences the electronic structure, because real polysilane systems are an aggregative form of many polysilane chains or have been reported to form polymeric crystalline structures. We then investigate the electronic structure of two-dimensional planar model polysilane by taking into account influences due to interlayer interaction. Based on these results for chain polysilane (1D) and planar polysilane (2D), we qualitatively discuss how the sterical dimension of Si skeletons modify the shapes of electronic structures.

II. LDF CALCULATION METHOD

This section outlines the LDF calculation method.[11-14] When $\Psi^{\sigma}_{\mu,\mathbf{k}}(\mathbf{r})$ represents the eigenstate with σ-spin state in the μth band having a $\mathbf{k}$-wave vector at point $\mathbf{r}$, total electron energy is given in the following form:

$$E_{\text{total}}=\sum_{\text{occ}}\int\Psi^{*\sigma}_{\mu,\mathbf{k}}(\mathbf{r})(-\tfrac{1}{2}\nabla^2)\Psi^{\sigma}_{\mu,\mathbf{k}}(\mathbf{r})d\mathbf{r}+\int\left[\sum_{l,\beta}V^{\beta,\text{local}}_{\text{ion}}(\mathbf{r}-\mathbf{R}_l-\tau_\beta)\right]\rho(\mathbf{r})d\mathbf{r}$$
$$+\sum_{\text{occ}}\int\Psi^{*\sigma}_{\mu,\mathbf{k}}(\mathbf{r})\left[\sum_{L,l,\beta}V^{\beta,\text{nonlocal}}_{\text{ion},L}(\mathbf{r}-\mathbf{R}_l-\tau_\beta)\hat{P}_L\right]\Psi^{\sigma}_{\mu,\mathbf{k}}(\mathbf{r})d\mathbf{r}+E_H+E_{\text{xc}}\ . \tag{1}$$

Here, we use Rydberg atomic units. $V^{\beta,\text{local}}_{\text{ion}}(\mathbf{r}-\mathbf{R}_l-\tau_\beta)$ and $V^{\beta,\text{nonlocal}}_{\text{ion}}(\mathbf{r}-\mathbf{R}_l-\tau_\beta)$ represent the local and nonlocal parts of the pseudopotential of the ion β positioned at $\mathbf{R}_l+\tau_\beta$, where $\mathbf{R}_l$ and τ_β denotes the position vectors of the lth unit cell and ion β in a unit cell. $\hat{P}_L$ is the projection operator of angular momentum. E_H represents the Hartree energy due to valence electrons, which is calculated from the total valence charge density $\rho(\mathbf{r})$ as follows:

$$E_H=\tfrac{1}{2}\int\int\frac{\rho(\mathbf{r})\rho(\mathbf{r}')}{|\mathbf{r}-\mathbf{r}'|}d\mathbf{r}\,d\mathbf{r}'\ , \tag{2}$$

where

$$\rho(\mathbf{r})=\sum_{\text{occ}}|\Psi^{\sigma}_{\mu,\mathbf{k}}(\mathbf{r})|^2 . \tag{3}$$

Furthermore, E_{xc} represents the exchange-correlation energy, for which we adopt the functional form of Cerpley and Alder's[15] potential parametrized by Perdew and Zunger.[16] This approximation is known to yield reasonable results.

Total energy E_{total} has been minimized with respect to $\Psi^{\sigma}_{\mu,\mathbf{k}}$, subject to the normalization constraint on the orbitals. The well-known one-particle equation is obtained:

$$[-\tfrac{1}{2}\nabla^2+V^{\sigma}_{\text{total}}(\mathbf{r})]\Psi^{\sigma}_{\mu,\mathbf{k}}(\mathbf{r})=\varepsilon^{\sigma}_{\mu,\mathbf{k}}\Psi^{\sigma}_{\mu,\mathbf{k}}(\mathbf{r}) . \tag{4}$$

Here, we express the Bloch function $\Psi^{\sigma}_{\mu,\mathbf{k}}(\mathbf{r})$ by the LCAO form

$$\Psi^{\sigma}_{\mu,\mathbf{k}}(\mathbf{r})=\frac{1}{\sqrt{\Omega}}\sum_{l,\alpha}e^{i\mathbf{k}\cdot\mathbf{R}_l}C^{\alpha,\sigma}_{\mu,\mathbf{k}}\chi^{\alpha}(\mathbf{r}-\mathbf{R}_l-\tau_{\alpha}) , \tag{5}$$

where χ^{α} is an atomic orbital of type α $(=s,p,d,\ldots)$ situated at τ_{α}. Using this expansion, the one-particle equation is reduced to the following self-consistent eigenvalue equation:

$$\sum_{\beta}(T^{\mathbf{k}}_{\alpha,\beta}+V^{\mathbf{k},\sigma}_{\alpha,\beta})C^{\beta,\sigma}_{\mu,\mathbf{k}}=\varepsilon^{\sigma}_{\mu,\mathbf{k}}\sum_{\beta}S^{\mathbf{k}}_{\alpha,\beta}C^{\beta,\sigma}_{\mu,\mathbf{k}} . \tag{6}$$

Here, $T^{\mathbf{k}}_{\alpha,\beta}$ is the kinetic energy and $V^{\mathbf{k}\sigma}_{\alpha,\beta}$ is the total potential energy which is separated into a local part and a nonlocal part. $S^{\mathbf{k}}_{\alpha,\beta}$ is the overlap matrix. In diagonalizing this equation, we first obtain the energy eigenvalue and wave function for each $\mathbf{k}$ point. From these, we can calculate the charge density, from which Hartree and exchange-correlation potential in the next iteration step can be calculated. This self-consistent-field (SCF) procedure is repeated until convergence is achieved. In practical calculations, we set the condition of SCF as

$$\int|V^{(n)}_{\text{total}}(\mathbf{r})-V^{(n+1)}_{\text{total}}(\mathbf{r})|^2d\mathbf{r}\le 1.0\times10^{-10}\ \text{Ry}^2 . \tag{7}$$

Here, we use the norm-conserving pseudopotential introduced by Hamann *et al.*[17] in which the core basis functions are neglected for calculation. This pseudopotential satisfies the following conditions.

(1) The pseudowave function is nodeless.

(2) The pseudopotential reproduces the atomic energy levels which are calculated by all electron calculations within the local-density-approximation (LDA) scheme.

(3) The pseudowave functions and the atomic wave functions have the same value outside the core region.

From these conditions, the valence charge density outside the core region is the same both for pseudowave functions and atomic wave functions.

In the LCAO calculation, the choice of atomic basis functions is very important. In this calculation we express the pseudoatomic wave function of chosen atomic configuration obtained numerically in terms of the sum of Gaussian-type orbitals[13,14] (GTO's) as

$$\chi^{\alpha}_{\text{GTO}}(\mathbf{r}-\mathbf{R}_l-\tau_{\alpha})=|\mathbf{r}-\mathbf{R}_l-\tau_{\alpha}|^{L_{\alpha}}\left\{\sum_i c_i e^{-\alpha_i|\mathbf{r}-\mathbf{R}_l-\tau_{\alpha_i}|^2}\right\}\times Y^{M_{\alpha}}_{L_{\alpha}}(\mathbf{r}-\mathbf{R}_l-\tau_{\alpha}) . \tag{8}$$

We determine the parameters of expansion coefficients c_i and Gaussian exponent α_i by the least-squares-fit method. Then we use each Gaussian orbital of exponent α_i as a basis function. These GTO bases accurately reproduce a consistent band structure of crystalline Si having an indirect band gap of 0.7 eV. Table I shows the values of Gaussian exponents in this calculation. For the present Brillouin-zone integral, we choose two special points for the 1D irreduced Brillouin zone and nine points for the 2D irreduced Brillouin zone.

TABLE I. Gaussian exponents of Si 3*s* Si 3*p* and H 1*s* AO's.

Atomic orbitals	α_1	α_2	α_3
Si 3*s*	0.9764	0.3070	0.1009
Si 3*p*	0.3215	0.1114	
H 1*s*	1.3325	0.201 53	

III. 1D Si-SKELETON MATERIALS

A. Polysilane chain

Figure 1 shows the resulting energy-band structure for transplanar zig-zag parent-polysilane $(SiH_2)_n$ with D_{2h}

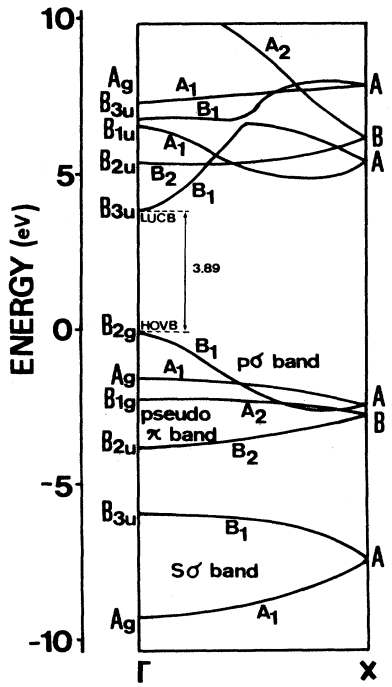

FIG. 1. Electronic structure of isolated polysilane chain $(SiH_2)_n$ with transplanar D_{2h} symmetry. Energy scale is represented from HOVB in eV.

point-group symmetry. Both of the band-edge states, the highest occupied valence band (HOVB) and the lowest unoccupied conduction band (LUCB), are located at point Γ. The LDF band calculation also results in a directly-allowed-type band structure with a band gap of 3.89 eV. The shape of the valence-band structure agrees with our previous semiempirical[6] and *ab initio*[5,10] results, and also with the other LDF result by Mintmier *et al.*[18] The orbital characters of the present valence bands are also in agreement with those previous ones. For convenience, here we call them $s\sigma$, pseudo-π, and $p\sigma$ bands, based on their orbital characters at point Γ.[7] The resulting HOVB state is formed by the bonding state between Si $3p_x$ orbitals (directed to the skeleton axis). This HOVB state is well delocalized along the skeleton. The LDF band structure also reproduces the characteristic isolation of the pseudo-π band from the $p\sigma$ band.

The characteristics of electron delocalization in conduction bands (CB's) or excited states are slightly different from our previous semiempirical results.[7] An increase in E-**k** dispersion means an increase in electron delocalization in CB's. This causes bands to overlap. The significant difference from the semiempirical results is an increase in the bandwidth of the pseudo-π^* band (B_{2u}-B_2-B-A_2-B_{1g} in CB's); it is about 6 eV, about five times larger than the semiempirical one. The present LDF calculation well describes this larger bandwidth, because bases in this work are refined from *ad hoc* ones in our previous semiempirical calculations. The resulting LUCB state has an irreduced representation the same as the previous results (B_{3u}). The orbital character, however, seems to be different from our previous semiempirical one: This LDF method results in a *sp* hybridized state having a strong $p\sigma^*$ antibonding character between neighboring Si $3p_y$ orbitals. On the contrary, our previous semiempirical method gave an almost $s\sigma^*$ antibonding state between Si $3s$ orbitals. Considering that semiempirical calculation gives the hybridization ratio qualitatively not quantitatively, the true LUCB orbital character would be well described by the present LDF result rather than by our previous ones. *Ab initio* band calculation[10] also gives a similar *sp* hybridized orbital character for LUCB state.

B. Interchain interaction

The effect of interchain interaction on the electronic structure has been discussed by approaching chains transversely (z direction) and longitudinally (y direction) as shown in Fig. 2(a). The most closed chains configuration is assumed to be the van der Waals (VDW) contacting geometry, where side-chain H atoms of neighboring chains are transversely and longitudinally contacting with the VDW length, respectively [Figs. 2(b) and 2(c)].

Interchain interaction, due to approaching chains transversely, appears significantly in π-like bands [screened bands in Fig. 3(a)]. The transverse interchain interaction lifts these bands upwards while conserving the E-**k** dispersion along the skeleton; e.g., the resulting

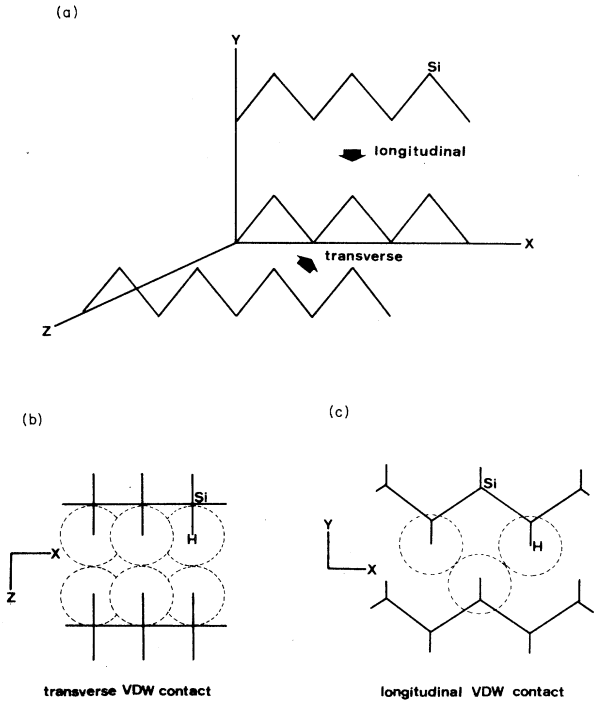

FIG. 2. Configuration of (a) transverse and longitudinal chains and (b) their transverse and (c) longitudinal VDW contacting geometry.

pseudo-π band finally rises so as to overlap the $p\sigma$ band perfectly for a transverse VDW contacting geometry. This band destabilization can qualitatively be interpreted by investigating the phase relationship among the corresponding eigenstates. In the pseudo-π band, side-chain H atoms are bonded to the skeleton Si $3p_z$ through $sp\sigma$ bonding. When chains are transversely closed, an antibonding phase relation is inevitably produced among H $1s$ orbitals of the neighboring chains [Fig. 3(b)]. This antibonding phase configuration destabilizes the on-site energy of side-chain H $1s$ orbitals. Since skeleton Si $3p_z$ orbitals hybridize with those destabilized H $1s$ orbitals in order to form the pseudo-π band, the resulting pseudo-π band should be lifted upwards. However, the interchain length, even for VDW contacting geometry, is large enough to change little in the *intrachain interaction* between Si $3p_z$ orbitals. This small change hardly modifies E-**k** dispersion in π-like bands. This is the reason why the pseudo-π band is lifted upwards while conserving the dispersion along the skeleton. The pseudo-π^* band is also lifted by a similar mechanism. Thus, the transverse interchain interaction appears through the destabilization of the on-site energy of the side groups (H atoms). However, this type of transverse interchain interaction disappears when two chains are over 8 Å apart.

Longitudinal interchain interaction lifts the LUCB state (B_{3u}). This lifting effectively increases a value of the direct band gap [Fig. 4(a)]. The orbital character of B_{3u} state is the *sp* hybridized state having strong Si $3p_y$ character. The corresponding orbital phase relationships are

shown in Fig. 4(b). The longitudinal approach of another chain produces the antibonding phase configuration among Si $3p_y$ orbitals of the neighboring chains. This type of orbital phase configuration destabilizes the B_{3u} eigenstate and lifts its own state upward. For a longitudinal VDW contacting geometry, the B_{3u} state is finally located at the energy state higher than that of point $*$ on the Δ axis. In this situation, the LUCB state is not at point Γ but at point $*$. The resulting energy-band structure changes from a direct type to an indirect type, which is optically inactive. Thus, if polysilane chains can be longitudinally closed by pressure, etc., the following optical phenomena might be expected: first a blue shift in an absorption edge caused by an increase in a band gap and then an absorption tail originating from an indirect transition might appear above a critical pressure in the ideal case. The longitudinal interchain interaction is also found as a slight upward shift of the HOVB (B_{2g}) state and as an expanding of the $s\sigma$ band. However, this interaction hardly affects such band states delocalizing toward the z direction (π-like bands).

Interchain interaction works on different band states depending on a sterical chains geometry; transverse interchain interaction modifies π-like states. The σ states are modified by longitudinal interchain interaction. Therefore, electronic states near the band edges, in particular

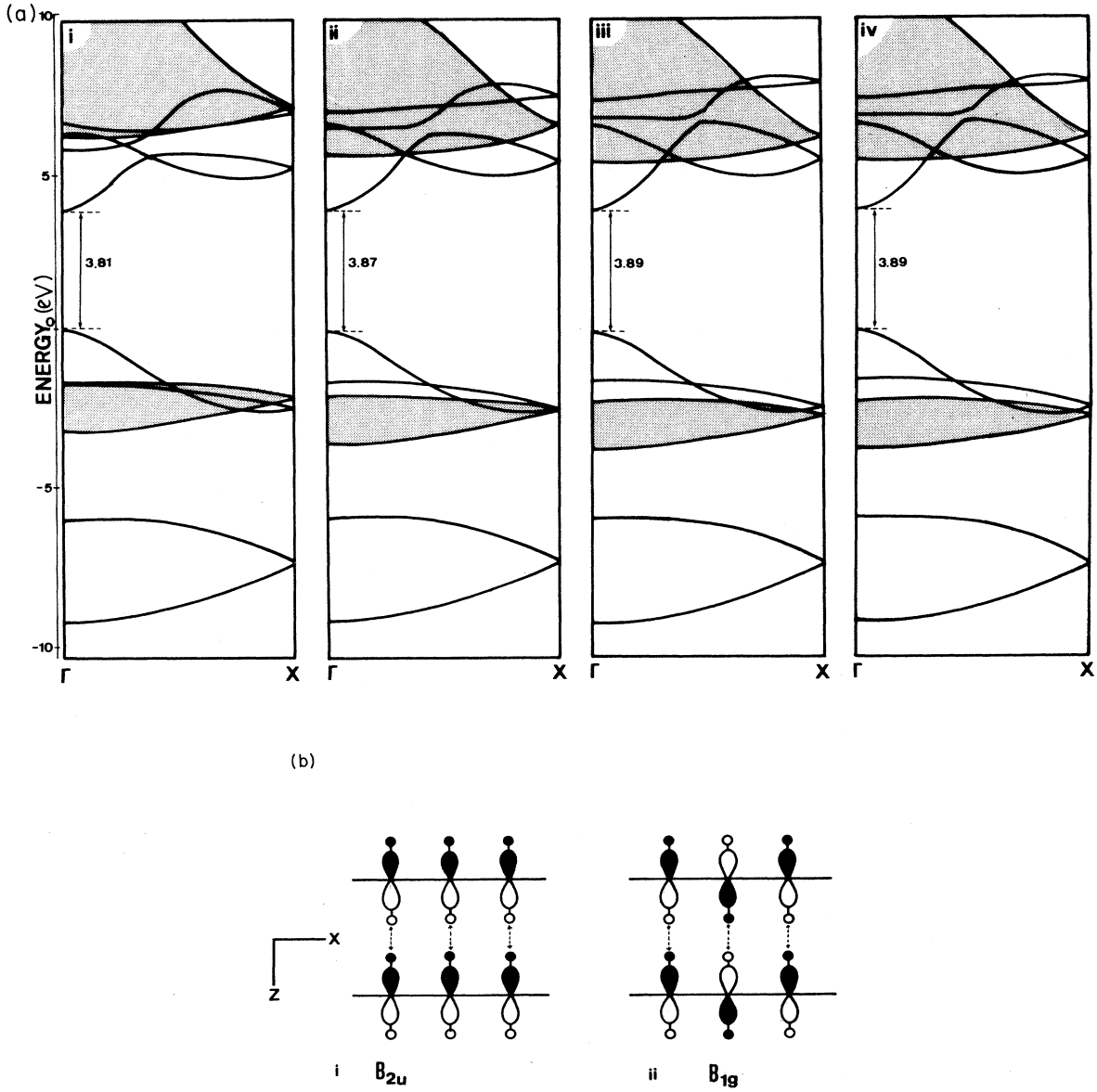

FIG. 3. (a) Change in band structure due to transverse interchain interaction, two chains are transversely configured with (i) VDW contacting length, (ii) 5.7 Å, (iii) 7.6 Å, and (iv) 9.5 Å. Energy scale is represented from HOVB in eV. (b) Phase relation between AO's of neighboring chains for (i) B_{2u} state and (ii) B_{1g} state of pseudo-π band.

the LUCB state, are influenced by longitudinal interchain interaction rather than by transverse interaction for this present chains geometry. Strong longitudinal interchain interaction might change the band structure from a direct type to an indirect type. However, interchain interaction disappears, if each chain is located over 8 Å from other chains, independently of the chain configurations. The reason is that polysilane is a typical nonpolar high polymer. Here, we divided interchain interaction into two modes, transverse and longitudinal. This artificial division is helpful in discussing the influence of the crystallization of polysilane chains on its electronic structure (in the next section), because polymeric crystal has both transverse and longitudinal interchain interactions simultaneously.

C. Crystalline polysilane chains

It is well known that some polymer chains form a polymeric crystalline structure. Polysilanes are not an exception for such polymers; e.g., dihexylpolysilane has been reported to form a monoclinic structure of $a=13.75$, $b=21.82$, $c=4.07$ Å, and $\gamma=88°$ by x-ray

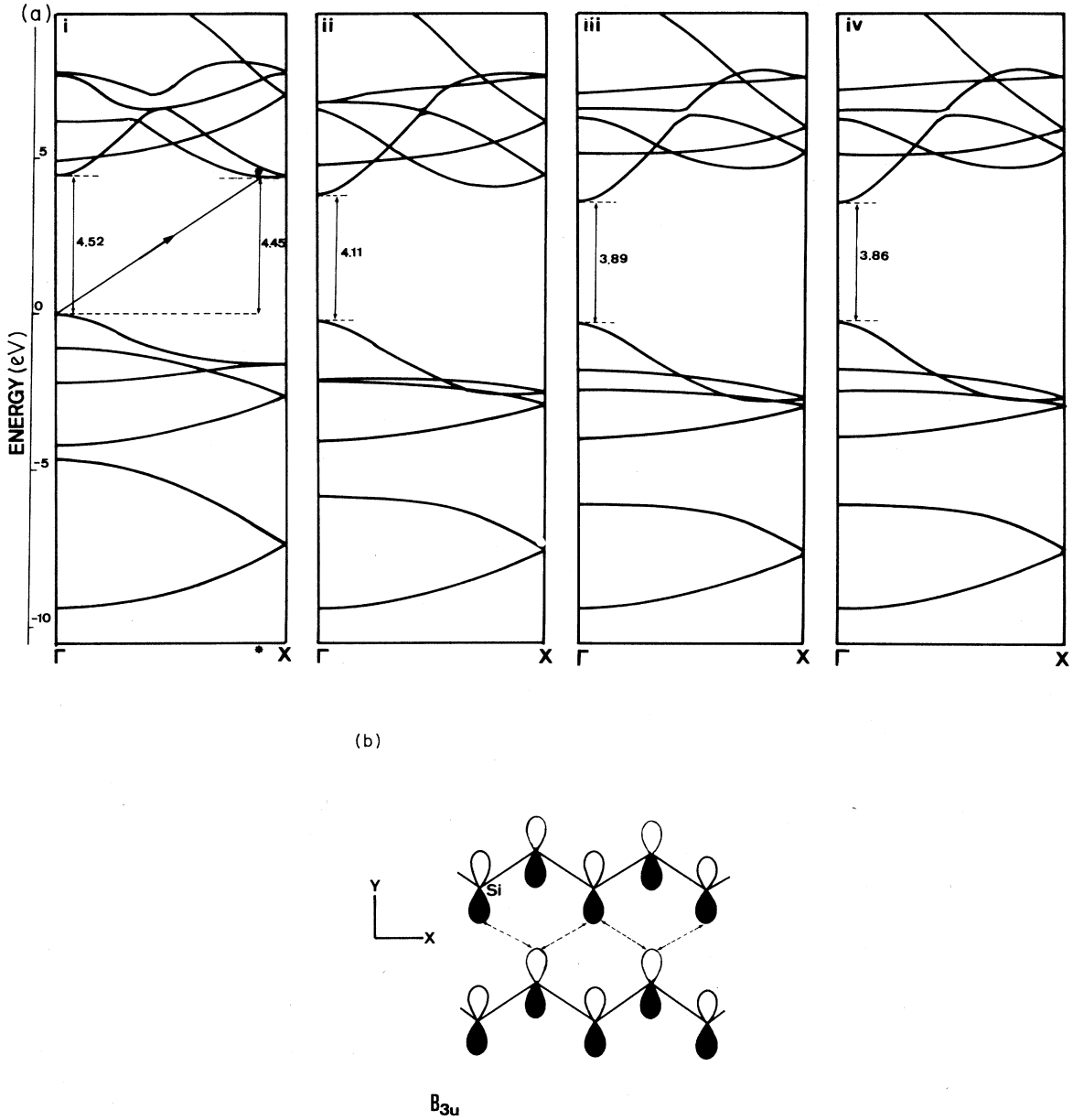

FIG. 4. (a) Change in band structure due to longitudinal interchain interaction; two chains are longitudinally configured with (i) VDW contacting length, (ii) 4.9 Å, (iii) 7.6 Å, and (iv) 9.5 Å. Energy scale is represented from HOVB in eV. (b) Phase relation between AO's of neighboring chains for the lower B_{3u} state in CB's.

diffraction experiments.[19] Based on these results, Miller *et al.*[20] concluded that the characteristic thermochromism of dihexylpolysilane observed at about room temperature is caused by the structure phase transition between amorphous and crystalline phases.

Here, we theoretically discuss the influence due to the crystallization of polysilane chains on the electronic structure. Parent polysilane $(SiH_2)_n$ with D_{2h} symmetry is considered as a model polysilane chain. These polysilane model chains are assumed to form an orthorhombic crystalline structure having *Pnam* symmetry similar to polyethylene (C analogue of parent polysilane),[21] because of the similar nonpolarity in parent polysilane and polyethylene. The resulting hypothetical lattice has lattice vectors of $a=9.98$, $b=6.65$, and $c=3.81$ Å. Those values are deduced from the real structure of polyethylene[21] in taking into account similar magnification by the ratio of the corresponding covalent bond lengths of silicon and carbon. Figure 5 shows the orthorhombic model crystal of parent polysilane chains with *Pnam* structure. Although dihexylpolysilane has been reported not to form an orthorhombic structure but a monoclinic one and also to have its side chain composed of not a H atom but a hexyl group, some characteristics of the electronic structure can be obtained by analogy from the results for this model crystal by the following reasons. First, the corresponding crystal structures are similar. The monoclinic dihexylpolysilane polymer crystal has a crystal angle of $\gamma=88°$, which is nearly equal to that for an orthorhombic model crystal ($\gamma=90°$). Second, the side-chain substitution causes little inherent change in the shape of band-edge electronic structure, because the *skeleton–side-chain* interaction is not significant in alkylpolysilanes.[8]

Figure 6 shows the calculated electronic structure of orthorhombic crystalline polysilane. Directly-allowed-type band structure is conserved even when polysilane chains are arranged to form a polymeric crystal with *Pnam* symmetry. Slight state resolution occurs in the pseudo-π band. Two pseudo-π bands result along the Δ axis ($\Gamma-Z$). This band splitting is caused by comparative delocalization of pseudo-π-band electrons towards the x-y plane. However, it is important that the outline of the valence-band structure along this direction is similar to that for isolated chains.

The interchain interaction due to orthorhombic crystallization can be well interpreted by investigating the E-$\mathbf{k}$ dispersion towards $\Gamma-X$ and $\Gamma-Y$. States of Γ_3 and Γ_4 correspond to B_{2u} and B_{1g} states of the isolated chain pseudo-π band, respectively. Since the unit cell involves two independent chains, the corresponding energy eigenstates should be degenerate, if these two chains do not interact at all. Crystallization resolves the degeneracy of these two states and splits each of them into two states of additional bonding and antibonding ones. Four states of Γ_3^b and Γ_3^a, and also Γ_4^b and Γ_4^a result. This additional bonding state (Γ_3^b or Γ_4^b) smoothly connects to the corresponding additional antibonding state (Γ_3^a or Γ_4^a) through the dispersion along $\Gamma-X$ or $\Gamma-Y$. The in-plane Si $3p$ character, due to the hybridization with Si $3p_x$ and Si $3p_y$, also causes a similar state splitting at Γ_5.

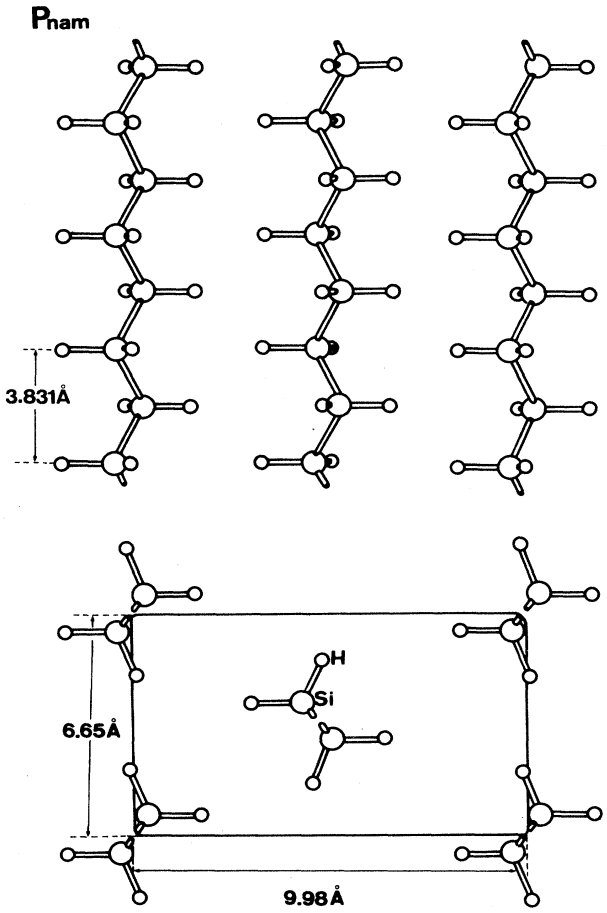

FIG. 5. Illustration of the orthorhombic polymer crystal model for parent polysilane chains.

The conduction-band states are influenced and different from those for an isolated chain. As previously discussed, electrons in CB's tend to delocalize. This induces a comparatively strong interchain interaction. Therefore, not only the pseudo-π^* band but also other bands are influenced by the interchain interaction due to polymeric crystallization of polysilane chains; even the LUCB state slightly splits into two states. This state resolution at the band edge principally produces the double band gaps. Shoulder peak structure observed at the absorption edge for dihexylpolysilane might originate from these double band gaps, because this shoulder peak can be found only in the crystalline phase. The calculated energy difference between the absorption edge and shoulder peak (about 0.11 eV) seems to be compatible with the observed one (0.06 eV).[22–24]

Thus, influence due to polymer crystallization of polysilane chains appears through the interchain interaction. However, this effect is small compared with that due to the intrachain interaction toward the skeleton chain axis. The reason is that polymeric crystallization of nonpolar polysilane chains produces a large *interspace* between chains. Therefore, the electronic structure near

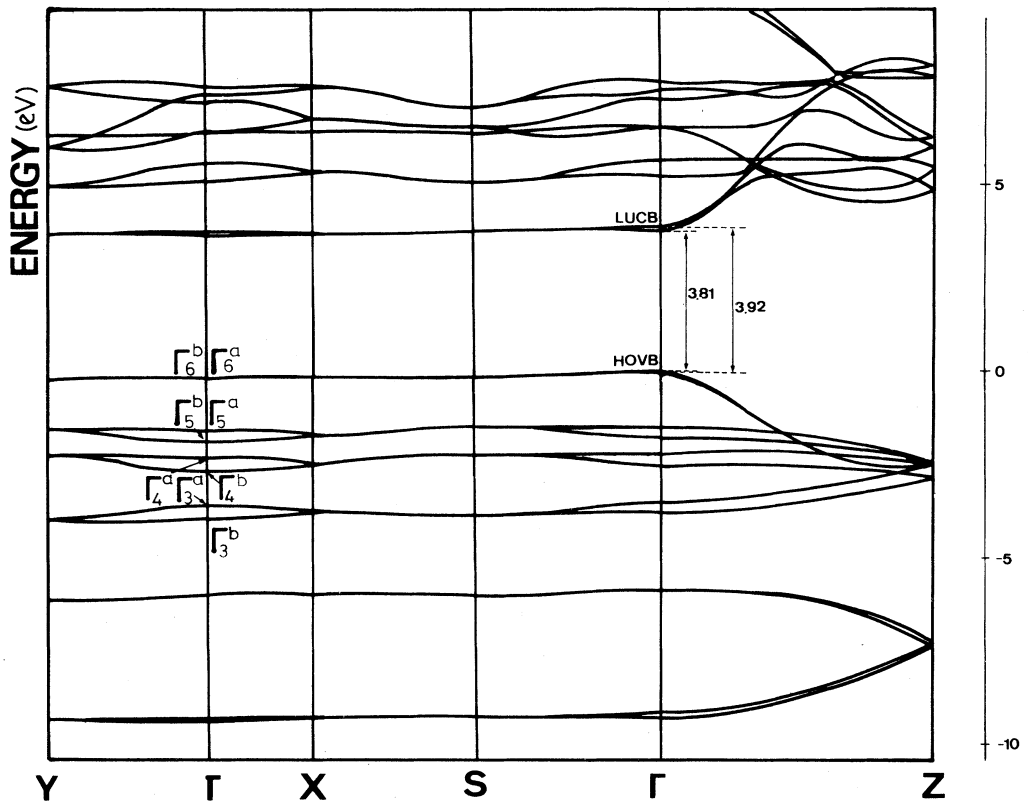

FIG. 6. Resulting electronic structure for orthorhombic crystalline polysilane chains. Energy scale is represented from HOVB in eV.

the band edges can be discussed in terms of the result for isolated polysilane chains, except for the double-band-gap structure. The resulting strong dispersion toward the skeleton axis would conclude the band conduction of carriers when an electric field is applied parallel to the skeleton axis. On the contrary, hopping controls the carrier conduction when the electric field is applied vertically to the skeleton axis, because of little dispersion toward the direction horizontal to the skeleton axis.

IV. 2D Si-SKELETON MATERIALS

A. Planar polysilane

Recently, Weidman *et al.*[4] have reported synthesizing two-dimensionally (2D) bonded Si-skeleton network polysilanes having alkyl side chains R (= *n*-propyl,*n*-butyl,*n*-hexyl). Ubara *et al.* have also reported a 2D amorphous Si.[3] Here, we theoretically investigate the electronic structure of 2D network polysilanes. Since a detailed structure analysis of these 2D Si-network polysilanes has not been made yet, a chair-type hexagonal Si-skeleton network structure is assumed in this work, because we intend to focus on saturated Si-skeleton 2D high polymers [Fig. 7(a)]. For a simplification, all alkyl side chains are substituted for H atoms. This substitution inherently produces little change in the shape of the band structure.[7,8] Interatomic bond lengths are quoted from the reported covalent bond lengths.[25] The resulting lattice vectors, $\mathbf{a}_1$ and $\mathbf{a}_2$ are given as

$$\mathbf{a}_1=\tfrac{1}{2}a(\mathbf{x}-\sqrt{3}\mathbf{y}) , \tag{9}$$

$$\mathbf{a}_2=\tfrac{1}{2}a(\mathbf{x}+\sqrt{3}\mathbf{y}) \tag{10}$$

with $a=3.831$ Å. Two Si atoms and two side-chain H atoms are included in the unit cell. The reciprocal-lattice vectors, $\mathbf{b}_1$ and $\mathbf{b}_2$, are given as

$$\mathbf{b}_1=\frac{2\pi}{a}\left[\mathbf{x}-\frac{1}{\sqrt{3}}\mathbf{y}\right] \tag{11}$$

$$\mathbf{b}_2=\frac{2\pi}{a}\left[\mathbf{x}+\frac{1}{\sqrt{3}}\mathbf{y}\right] . \tag{12}$$

Figure 7(b) shows the corresponding Brillouin zone.

Figure 8 shows the calculated band structure. 2D planar polysilane has two characteristic band gaps: an indirect one of 2.48 eV and a direct one of 2.63 eV. 1D chain polysilane conserves the directly-allowed-type band structure even when chains form a polymer crystalline structure. Conversely, the electronic band structure of 2D planar polysilane has an energy structure similar to the indirect one of 3D crystal Si rather than the direct one of 1D chain polysilane. However, the difference from 3D crystal Si is that the two characteristic band gaps of 2D planar polysilane give similar values. One could then

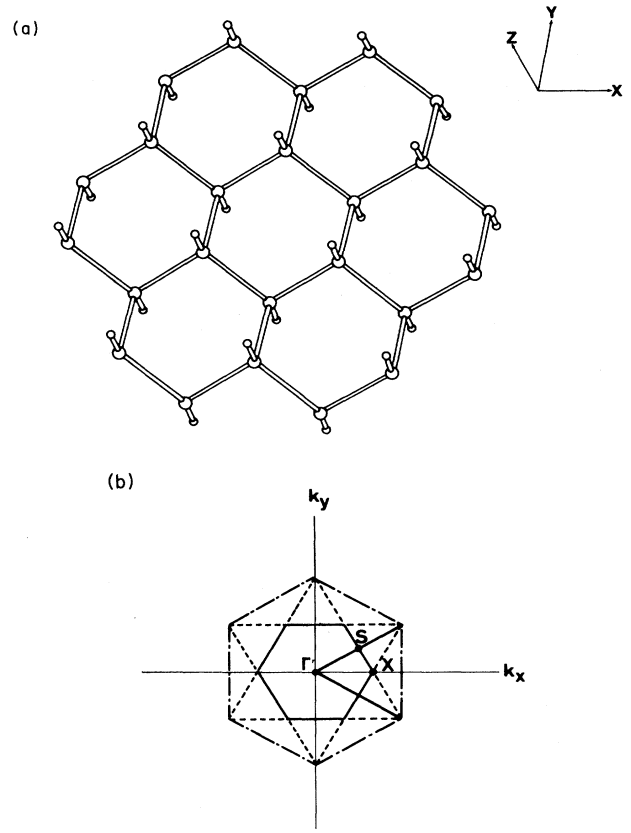

FIG. 7. (a) 2D planar polysilane $(SiH)_n$ and (b) its Brillouin zone.

call the band structure of 2D planar polysilane a mixed band-gap structure having direct and indirect band gaps. This mixed band-gap structure might cause a characteristic optical-absorption edge; a weak tail edge due to indirect transition and a strong edge originating from direct transition. A steplike profile[4] is also expected because of two dimensionality.

HOVB state is doubly degenerate and both states are delocalized in the skeleton plane (x-y plane); these degenerate states are formed of $p\sigma$ bonding states between Si $3p_x$ orbitals or between Si $3p_y$ orbitals. Since the Si $3p_z$ orbital stands vertically on the skeleton plane, this orbital does not degenerate with the above two $p\sigma$ states but hybridizes with side chain H $1s$ orbitals so as to stabilize. This stabilization lowers the eigenstate about 2.6 eV below the above $p\sigma$ HOVB states. When Si-skeleton networking proceeds toward such direction vertical to the skeleton plane, the 3D characteristic of c-Si begins to appear. In this situation, the $p\sigma$-bonding state between Si $3p_z$ orbitals tends to close to the above doubly degenerate $p\sigma$ HOVB states. Finally, these three states will degenerate at point Γ to form threefold-degenerate HOVB states of 3D crystalline Si.

Thus, neglecting the spin and spin-orbit interaction, HOVB states are singly, doubly, or triply degenerate, depending on the structure dimension of the 1D, 2D, or 3D Si skeleton, respectively. However, the orbital character of HOVB state is Si $3p\sigma$ bonding independent of the structure dimension. Resulting states tend to delocalize toward the Si-skeleton direction, i.e., the skeleton axis for 1D chain polysilanes, the skeleton plane for 2D planar polysilanes, and the skeleton bonds for 3D crystalline sil-

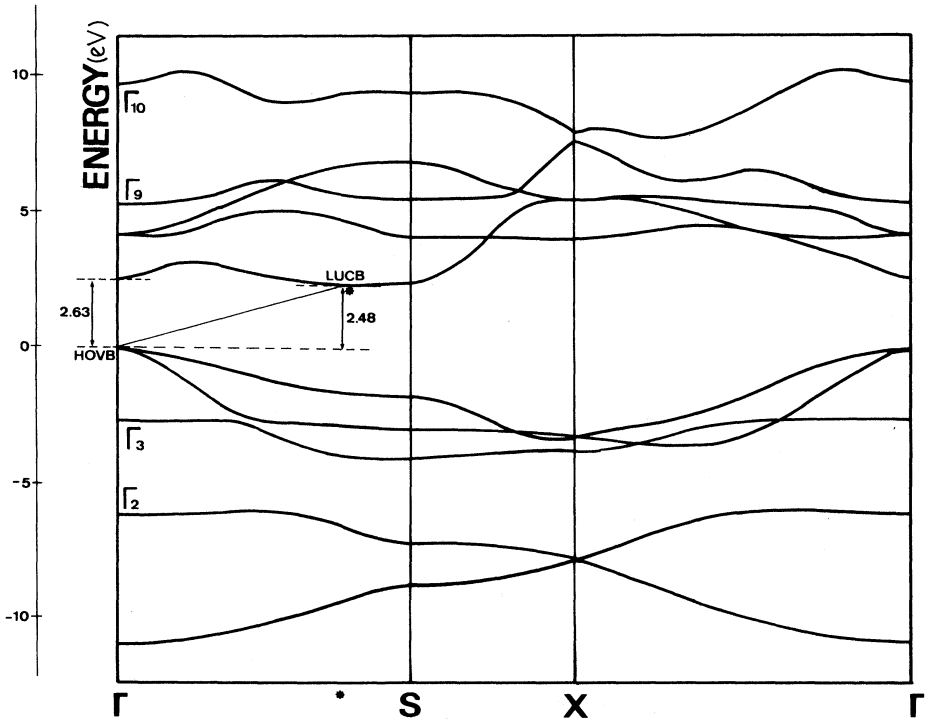

FIG. 8. Calculated electronic structure for 2D planar polysilane. Energy scale is represented from HOVB in eV.

icon.

The lower unoccupied state at point Γ gives σ^* antibonding character between skeleton Si 3s orbitals. This state also delocalizes in the skeleton plane. It is confirmed by the strong dispersion near point Γ. Since 2D polysilane has such Si skeletons that effectively induce the longitudinal interchain interaction, the energy eigenvalue at point * on the Δ axis is situated 0.15 eV lower than that at point Γ. This is the origin of the indirect band structure of 2D planar polysilane. Doubly degenerate in-plane Si $3p\sigma^*$ states can be also found in the conduction band. These states correspond to the antibonding part of HOVB states.

B. Interlayer interaction

When other 2D polysilanes are arranged to contact by the VDW contacting length, the energy-band structure changes as shown in Fig. 9. HOVB states are hardly changed even by this strong closing of other 2D planar polysilanes. The lowest unoccupied states along the Δ axis tend to lower their energy eigenvalues slightly. Therefore, the direct and indirect band gaps decrease from 2.63 eV (isolated 2D layer) to 2.46 eV (VDW contacting layers) and from 2.48 to 2.34 eV, respectively. This slight decrease also blurs the difference between the direct and indirect gaps. However, the corresponding changes are not remarkable, and it can be said that band-edge states are hardly influenced by interlayer interaction even for the VDW contacting arrangement. This can be confirmed in terms of nondispersion along the Γ–Z (out-of-plane) direction. The reason is that these band-edge states delocalize toward the in-plane direction but localize toward the out-of-plane direction.

Stronger interlayer interaction is expected in the electronic states delocalizing toward the out-of-plane direction. These states correspond to π-like states formed of skeleton Si $3p_z$ orbitals or diffusive states toward horn H atoms. Although interlayer interaction appears via horn H atoms, it gives an opposite influence on these states: The former states (Γ_3 and Γ_{10}) tend to be stabilized and the latter (Γ_2 and Γ_9) to be destabilized. This is because, with the closing of other 2D polysilane layers, a bonding character among H 1s orbitals of neighboring layers is strengthened (the former states) but an antibonding character among them is enhanced (the latter states).

V. CONCLUSION

The LDF band calculation for chain (1D) polysilane gives a direct-type band structure with 3.89 eV gaps.

Interchain interaction works on different band states depending on a sterical chain geometry. Strong longitudinal interchain interaction results in a theoretical possibility to change the band structure from a direct type to an indirect type. However, interchain interaction disappears, independently of the chain configuration, if each chain is located over 8 Å from other chains.

1D chain polysilane conserves the directly-allowed-type band structure even when chains form a polymer crystalline structure. The corresponding structure near the band edges can be discussed in terms of the result for

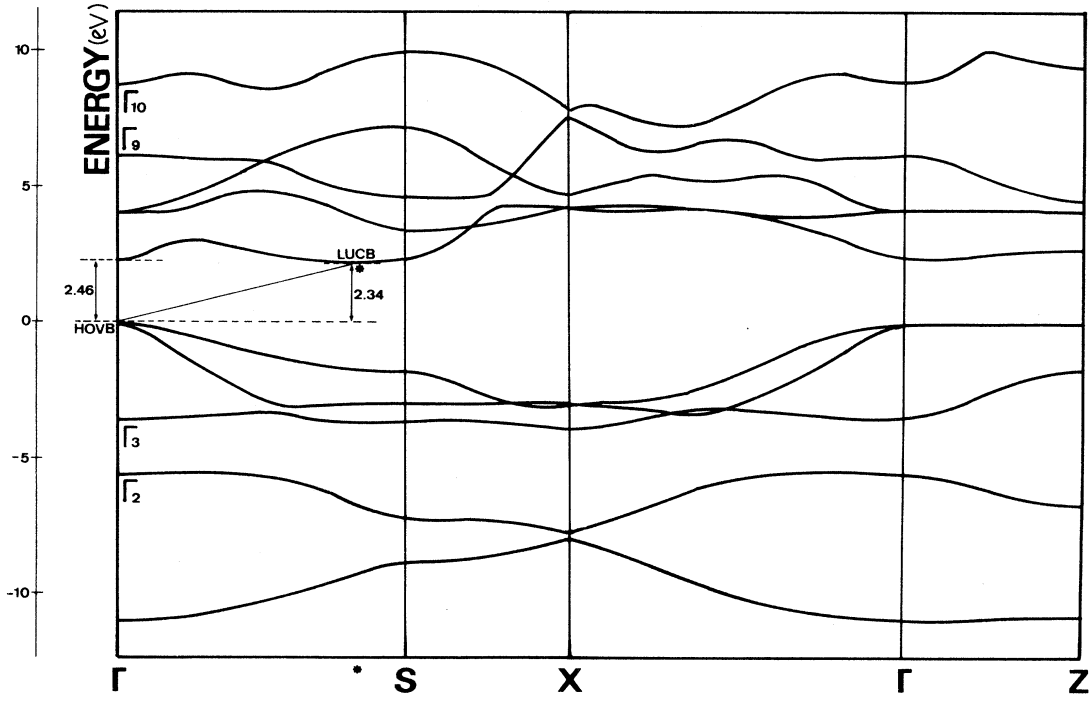

FIG. 9. Change in electronic structure for 2D planar polysilane. Two layers are configured with the VDW contacting length. Energy scale is represented from HOVB in eV.

the isolated polysilane chain, except for the double-band-gaps structure.

2D planar polysilane has a mixed-band-gap structure consisting of an indirect one (2.48 eV) and a direct one (2.63 eV). This structure is an intermediary between the direct type (1D) and indirect type (3D). A characteristic single, double, or triple degeneracy is found at the HOVB state, depending on the structure dimension of a 1D, 2D, or 3D Si skeleton, respectively.

Interlayer interaction gives little influence on the band-edge states of 2D planar polysilane, because these states are delocalized in the skeleton plane.

ACKNOWLEDGMENTS

We acknowledge the valuable help in the LDF band calculation program from Professor H. Kamimura and Dr. N. Shima (University of Tokyo), Dr. T. Nakayama (Chiba University), and also Dr. A. Oshiyama (NEC). We also express our thanks to Dr. T. Ohno, Dr. N. Matsumoto, Dr. M. Fujino, Dr. H. Teramae, and Dr. H. Isaka (NTT) for valuable discussions. Numerical calculations were performed at the NTT Super Computer Center (GIJHO).

[1]For a review, see R. West, J. Organometal. Chem. **300**, 327 (1986).

[2]N. Matsumoto, K. Takeda, H. Teramae, and M. Fujino, *Advances in Silicon-based Polymer Science* (in press).

[3]H. Ubara, T. Imura, A. Hiraki, I. Hirabayashi, and K. Morigaki, J. Non-Cryst. Solids **59&60**, 641 (1983).

[4]T. W. Weidman, P. A. Bianconi, and F. C. Schilling, Bull. Am. Phys. Soc. **33**, 541 (1988).

[5]H. Teramae, T. Yamabe, and A. Imamura, Theor. Chim. Acta **1**, 64 (1983).

[6]K. Takeda, N. Matsumoto, and M. Fukuchi, Phys. Rev. B **30**, 5871 (1984).

[7]K. Takeda, H. Teramae, and N. Matsumoto, J. Am. Chem. Soc. **108**, 8186 (1986).

[8]K. Takeda, M. Fujino, K. Seki, and H. Inokuchi, Phys. Rev. B **36**, 8129 (1987).

[9]J. T. Nelson and W. J. Pietro, J. Phys. Chem. **92**, 1365 (1988).

[10]H. Teramae and K. Takeda, J. Am. Chem. Soc. **111**, 1281 (1989).

[11]P. Hohenberg and W. Kohn, Phys. Rev. B **136**, 864 (1964).

[12]W. Kohn and L. J. Sham, Phys. Rev. **140**, A1133 (1965).

[13]A. Oshiyama and M. Saito, J. Phys. Soc. Jpn. **56**, 2104 (1987).

[14]K. Shiraishi, A. Oshiyama, N. Shima, T. Nakayama, and H. Kamimura, Solid State Commun. **66**, 629 (1988).

[15]D. M. Cerpley and B. J. Alder, Phys. Rev. Lett. **45**, 566 (1980).

[16]J. P. Perdew and A. Zunger, Phys. Rev. B **23**, 5048 (1981).

[17]D. R. Hamann, M. Schluter, and C. Chiang, Phys. Rev. Lett. **43**, 1494 (1979).

[18]J. W. Mintmire and J. Ortiz, in Proceedings of the International Topical Workshop on Advances in Si-bonded Polymer Science, Hawaii (to be published); Bull. Am. Phys. Soc. **33**, 540 (1988).

[19]H. Kuzmany, J. F. Rabolt, B. L. Farmer, and R. D. Miller, J. Chem. Phys. **85**, 7413 (1986).

[20]For a review, see J. F. Rabolt, Phys. Today, **41**, (1), S-67 (1988).

[21]C. W. Bunn, Trans. Faraday Soc. **35**, 482 (1939).

[22]R. D. Miller, D. Hofer, and J. Rabolt, G. N. Fickes, J. Am. Chem. Soc. **107**, 2172 (1985).

[23]H. Isaka (private communication).

[24]J. F. Rabolt, D. Hofer, R. D. Miller, and G. N. Fickes, Macromol. **19**, 611 (1986).

[25]J. C. Phillips, *Bonds and Bands in Semiconductors* (Academic, New York, 1973).